Comparison of multi-material phase retrieval methods with Edge illumination Single Mask and Free-Propagation

Information of the phase shift (ϕ) and the intensity associated with the absorption (I) are related to the real (δ) and imaginary (β) coefficients of the refractive index by means of the following equations

$$\phi\left(\frac{x}{M},\frac{y}{M},0,E\right) = -k(E)\int_{-z_o}^{0}\delta\left(\frac{x}{M},\frac{y}{M},z',E\right)dz' \tag{S1}$$

$$I\left(\frac{x}{M},\frac{y}{M},0,E\right) = I\left(\frac{x}{M},\frac{y}{M},-z_o,E\right)e^{-2k(E)\int_{-z_o}^{0}\beta\left(\frac{x}{M},\frac{y}{M},z',E\right)dz'} \tag{S2}$$

where M is the geometric magnification of the sample at the detector, E is the energy of X-rays through the sample, k is the wavenumber in vacuum and z_o is the thickness of the sample.

X-ray phase contrast methods

Edge illumination Single Mask: EISM

Characteristic equations: Two possible images constructed from an image in EISM, the first obeying equation S3 and the second obeying equation S4.

$$\frac{M^2 I_+(x,y,z_1,E)}{I_+\left(\frac{x}{M},\frac{y}{M},-z_o,E\right)} = e^{-2k(E)\int_{-z_o}^{0}\beta\left(\frac{x}{M},\frac{y}{M},z',E\right)dz'}\left[1+\frac{2z_1}{M_1Ak(E)}\frac{\partial\phi\left(\frac{x}{M},\frac{y}{M},0,E\right)}{\partial x'}\right] \tag{S3}$$

$$\frac{M^2 I_-(x,y,z_1,E)}{I_-\left(\frac{x}{M},\frac{y}{M},-z_o,E\right)} = e^{-2k(E)\int_{-z_o}^{0}\beta\left(\frac{x}{M},\frac{y}{M},z',E\right)dz'}\left[1-\frac{2z_1}{M_1Ak(E)}\frac{\partial\phi\left(\frac{x}{M},\frac{y}{M},0,E\right)}{\partial x'}\right] \tag{S4}$$

where M_1 is the geometric magnification of each aperture (A) from the EI mask, z_1 is the distance sample-detector, I_+ is the intensity given for one row of pixels and I_- is the intensity given for the neighboring row of pixels.

The traditional method of retrieving the absorption information in EISM is by adding equations 3 and 4 as:

$$e^{-2k(E)\int_{-z_o}^{0}\beta\left(\frac{x}{M},\frac{y}{M},z',E\right)dz'} = \frac{M^2}{2}\left[\frac{I_+(x,y,z_1,E)}{I_+\left(\frac{x}{M},\frac{y}{M},-z_o,E\right)}+\frac{I_-(x,y,z_1,E)}{I_-\left(\frac{x}{M},\frac{y}{M},-z_o,E\right)}\right] \tag{S5}$$

and the differential phase shift by subtracting equations 3 and 4 as:

$$\frac{\partial\phi\left(\frac{x}{M},\frac{y}{M},0,E\right)}{\partial x'} = \frac{M_1Ak(E)}{2z_1}\frac{\left[\frac{I_+(x,y,z_1,E)}{I_+\left(\frac{x}{M},\frac{y}{M},-z_o,E\right)}-\frac{I_-(x,y,z_1,E)}{I_-\left(\frac{x}{M},\frac{y}{M},-z_o,E\right)}\right]}{\left[\frac{I_+(x,y,z_1,E)}{I_+\left(\frac{x}{M},\frac{y}{M},-z_o,E\right)}+\frac{I_-(x,y,z_1,E)}{I_-\left(\frac{x}{M},\frac{y}{M},-z_o,E\right)}\right]} \tag{S6}$$

There are alternative phase retrieval methods in EISM that allow direct mapping of the projected thickness of each material within the sample. These include the Beltrán method.

- **Phase retrieval: Projected thickness maps**

The method starts with equations S1 and S2 within equations S3 and S4, obtaining

$$\frac{M^2 I_{\pm}(x,y,z_1,E)}{I_{\pm}\left(\frac{x}{M},\frac{y}{M},-z_o,E\right)} = e^{-2k(E)\int_{-z_o}^{0}\beta\left(\frac{x}{M},\frac{y}{M},z',E\right)dz'}\left[1 \mp \frac{2z_1}{M_1 A}\frac{\partial\int_{-z_o}^{0}\delta\left(\frac{x}{M},\frac{y}{M},z',E\right)dz'}{\partial x'}\right] \quad \textbf{(S7)}$$

The total projected thickness of the sample is defined as

$$a_T\left(\frac{x}{M},\frac{y}{M}\right) = a_1\left(\frac{x}{M},\frac{y}{M}\right) + a_2\left(\frac{x}{M},\frac{y}{M}\right) \quad \textbf{(S8)}$$

where the $a_1\left(\frac{x}{M},\frac{y}{M}\right)$ ($a_2\left(\frac{x}{M},\frac{y}{M}\right)$) refers to the projected thickness of the encasing (encapsulated) material. With equation S8 and the following approximation in the integral terms

$$\int_{-z_o}^{0}\delta\left(\frac{x}{M},\frac{y}{M},z',E\right)dz' = \delta_1(E)a_1\left(\frac{x}{M},\frac{y}{M}\right) + \delta_2(E)a_2\left(\frac{x}{M},\frac{y}{M}\right)$$

$$\int_{-z_o}^{0}\delta\left(\frac{x}{M},\frac{y}{M},z',E\right)dz' = \delta_1(E)a_T\left(\frac{x}{M},\frac{y}{M}\right) + \Delta\delta(E)a_2\left(\frac{x}{M},\frac{y}{M}\right) \quad \textbf{(S9)}$$

$$\int_{-z_o}^{0}\beta\left(\frac{x}{M},\frac{y}{M},z',E\right)dz' = \beta_1(E)a_1\left(\frac{x}{M},\frac{y}{M}\right) + \beta_2(E)a_2\left(\frac{x}{M},\frac{y}{M}\right)$$

$$\int_{-z_o}^{0}\beta\left(\frac{x}{M},\frac{y}{M},z',E\right)dz' = \beta_1(E)a_T\left(\frac{x}{M},\frac{y}{M}\right) + \Delta\beta(E)a_2\left(\frac{x}{M},\frac{y}{M}\right) \quad \textbf{(S10)}$$

where $\Delta\delta(E) = \delta_2(E) - \delta_1(E)$ and $\Delta\beta(E) = \beta_2(E) - \beta_1(E)$, equation S7 is written as

$$\begin{aligned}\frac{M^2 I_{\pm}(x,y,z_1,E)}{I_{\pm}\left(\frac{x}{M},\frac{y}{M},-z_o,E\right)} \\ = e^{-2k(E)\beta_1(E)a_T\left(\frac{x}{M},\frac{y}{M}\right)}e^{-2k(E)\Delta\beta(E)a_{2\pm}\left(\frac{x}{M},\frac{y}{M}\right)}\Bigg[1 \mp \frac{2z_1}{M_1 A}\delta_1(E)\frac{\partial a_T\left(\frac{x}{M},\frac{y}{M}\right)}{\partial x'} \\ \mp \frac{2z_1}{M_1 A}\Delta\delta(E)\frac{\partial a_{2\pm}\left(\frac{x}{M},\frac{y}{M}\right)}{\partial x'}\Bigg]\end{aligned} \quad \textbf{(S11)}$$

Assuming that the total projected thickness slowly varies along the transversal plane, then $\vec{\nabla}_T a_T\left(\frac{x}{M},\frac{y}{M}\right) \approx 0 \rightarrow \frac{\partial a_T\left(\frac{x}{M},\frac{y}{M}\right)}{\partial x'} \approx 0$. Although that assumption is violated at the edges of the sample, the retrieving of the projected thickness of the encapsulated material is valid only if it is not located close to the edges. Consequently, equation S11 is

$$\frac{M^2 I_{\pm}(x,y,z_1,E)}{I_{\pm}\left(\frac{x}{M},\frac{y}{M},-z_o,E\right) e^{-2k(E)\beta_1(E)a_T\left(\frac{x}{M},\frac{y}{M}\right)}} = e^{-2k(E)\Delta\beta(E)a_{2\pm}\left(\frac{x}{M},\frac{y}{M}\right)}\left[1 \mp \frac{2z_1\Delta\delta(E)}{M_1 A}\frac{\partial a_{2\pm}\left(\frac{x}{M},\frac{y}{M}\right)}{\partial x'}\right] \quad \textbf{(S12)}$$

$$\frac{M^2 I_{\pm}(x,y,z_1,E)}{I_{\pm}\left(\frac{x}{M},\frac{y}{M},-z_o,E\right) e^{-2k(E)\beta_1(E)a_T\left(\frac{x}{M},\frac{y}{M}\right)}} = \left[1 \pm \frac{z_1\Delta\delta(E)}{M_1 A k(E)\Delta\beta(E)}\frac{\partial}{\partial x'}\right] e^{-2k(E)\Delta\beta(E)a_{2\pm}\left(\frac{x}{M},\frac{y}{M}\right)} \quad \textbf{(S13)}$$

where $\frac{\partial}{\partial x'} e^{-2k(E)\Delta\beta(E)a_{2\pm}\left(\frac{x}{M},\frac{y}{M}\right)} = -2k(E)\Delta\beta(E)\frac{\partial a_{2\pm}\left(\frac{x}{M},\frac{y}{M}\right)}{\partial x'} e^{-2k(E)\Delta\beta(E)a_{2\pm}\left(\frac{x}{M},\frac{y}{M}\right)}$. Using Fourier space enables to convert the differential equations S13 into algebraic equations. Supposing a discrete system $N \times N$ pixels in the detector, with each pixel as a square of size W, the discrete Fourier transforms of each function from equation S13 are

$$F_{\pm}(x,y,E) = \frac{M^2 I_{\pm}(x,y,z_1,E)}{I_{\pm}\left(\frac{x}{M},\frac{y}{M},-z_o,E\right) e^{-2k(E)\beta_1(E)a_T\left(\frac{x}{M},\frac{y}{M}\right)}} = \frac{2}{N^2}\sum_{u=-\frac{N}{4}}^{\frac{N}{4}}\sum_{v=-\frac{N}{2}}^{\frac{N}{2}} f_{\pm}(u,v,E)e^{\frac{2\pi i}{N}(xu+yv)} \quad \textbf{(S14)}$$

$$G_{\pm}(x,y,E) = e^{-2k(E)\Delta\beta(E)a_{2\pm}\left(\frac{x}{M},\frac{y}{M}\right)} = \frac{2}{N^2}\sum_{u=-\frac{N}{4}}^{\frac{N}{4}}\sum_{v=-\frac{N}{2}}^{\frac{N}{2}} g_{\pm}(u,v,E)e^{\frac{2\pi i}{N}(xu+yv)} \quad \textbf{(S15)}$$

with u and v as the Fourier frequencies associated to x and y, respectively. A second-order Taylor expansion is used around the center of mass of an arbitrary pixel (x,y) to calculate the function $G_{\pm}$ in the center of mass of its neighbor pixels, at $(x \pm 2W, y)$, and the derivative of $G_{\pm}$ as

$$G_{\pm}(x \pm 2W, y, E) = G_{\pm}(x,y,E) \pm 2W\frac{\partial G_{\pm}(x,y,E)}{\partial x'} + \frac{4W^2}{2}\frac{\partial^2 G_{\pm}(x,y,E)}{\partial x'^2} \quad \textbf{(S16)}$$

$$\frac{\partial G_{\pm}(x,y,E)}{\partial x'} = \frac{1}{4W}\left[G_{\pm}(x+2W,y,E) - G_{\pm}(x-2W,y,E)\right] \quad \textbf{(S17)}$$

$$\frac{\partial G_{\pm}(x,y,E)}{\partial x'} = \frac{2}{4WN^2}\left[\sum_{u=-\frac{N}{4}}^{\frac{N}{4}}\sum_{v=-\frac{N}{2}}^{\frac{N}{2}} g_{\pm}(u,v,E)e^{\frac{2\pi i}{N}([x+2W]u+yv)} - \sum_{u=-\frac{N}{4}}^{\frac{N}{4}}\sum_{v=-\frac{N}{2}}^{\frac{N}{2}} g_{\pm}(u,v,E)e^{\frac{2\pi i}{N}([x-2W]u+yv)}\right] \quad \textbf{(S18)}$$

$$\frac{\partial G_{\pm}(x,y,E)}{\partial x'} = \frac{2}{4WN^2}\sum_{u=-\frac{N}{4}}^{\frac{N}{4}}\sum_{v=-\frac{N}{2}}^{\frac{N}{2}}\left[e^{\frac{2\pi i}{N}2Wu} - e^{-\frac{2\pi i}{N}2Wu}\right] g_{\pm}(u,v,E)e^{\frac{2\pi i}{N}(xu+yv)} \quad \textbf{(S19)}$$

$$\frac{\partial G_{\pm}(x,y,E)}{\partial x'} = \frac{2}{N^2}\sum_{u=-\frac{N}{4}}^{\frac{N}{4}}\sum_{v=-\frac{N}{2}}^{\frac{N}{2}} \frac{i}{2W}\sin\left(\frac{4\pi W u}{N}\right) g_{\pm}(u,v,E)e^{\frac{2\pi i}{N}(xu+yv)} \qquad \textbf{(S20)}$$

With equations S14, S15 and S20, equation S13 is expressed as

$$\frac{2}{N^2}\sum_{u=-\frac{N}{4}}^{\frac{N}{4}}\sum_{v=-\frac{N}{2}}^{\frac{N}{2}} f_{\pm}(u,v,E)e^{\frac{2\pi i}{N}(xu+yv)} = \frac{2}{N^2}\sum_{u=-\frac{N}{4}}^{\frac{N}{4}}\sum_{v=-\frac{N}{2}}^{\frac{N}{2}}\left[1 \pm \frac{iz_1\Delta\delta(E)}{2WM_1Ak(E)\Delta\beta(E)}\sin\left(\frac{4\pi W u}{N}\right)\right] g_{\pm}(u,v,E)e^{\frac{2\pi i}{N}(xu+yv)}$$

$$f_{\pm}(u,v,E) = \left[1 \pm \frac{iz_1\Delta\delta(E)}{2WM_1Ak(E)\Delta\beta(E)}\sin\left(\frac{4\pi W u}{N}\right)\right] g_{\pm}(u,v,E)$$

$$g_{\pm}(u,v,E) = \frac{f_{\pm}(u,v,E)}{1 \pm \frac{iz_1\Delta\delta(E)}{2WM_1Ak(E)\Delta\beta(E)}\sin\left(\frac{4\pi W u}{N}\right)} \qquad \textbf{(S21)}$$

allowing to calculate $a_{2\pm}\left(\frac{x}{M},\frac{y}{M}\right)$ from $g_{\pm}(u,v,E)$ in equations S15 as

$$e^{-2k(E)\Delta\beta(E)a_{2\pm}\left(\frac{x}{M},\frac{y}{M}\right)} = \frac{2}{N^2}\sum_{u=-\frac{N}{4}}^{\frac{N}{4}}\sum_{v=-\frac{N}{2}}^{\frac{N}{2}}\left[\frac{f_{\pm}(u,v,E)}{1 \pm \frac{iz_1\Delta\delta(E)}{2WM_1Ak(E)\Delta\beta(E)}\sin\left(\frac{4\pi W u}{N}\right)}\right] e^{\frac{2\pi i}{N}(xu+yv)}$$

$$a_{2\pm}\left(\frac{x}{M},\frac{y}{M}\right) = -\frac{1}{2k(E)\Delta\beta(E)}\ln\left[\frac{2}{N^2}\sum_{u=-\frac{N}{4}}^{\frac{N}{4}}\sum_{v=-\frac{N}{2}}^{\frac{N}{2}}\left[\frac{f_{\pm}(u,v,E)}{1 \pm \frac{iz_1\Delta\delta(E)}{2WM_1Ak(E)\Delta\beta(E)}\sin\left(\frac{4\pi W u}{N}\right)}\right] e^{\frac{2\pi i}{N}(xu+yv)}\right] \qquad \textbf{(S22)}$$

From equations S22, two estimates of the projected thickness of the encapsulated material can be obtained. Its total projected thickness can be estimated by averaging the two projected thicknesses as:

$$a_2\left(\frac{x}{M},\frac{y}{M}\right) = \frac{1}{2}\left[a_{2+}\left(\frac{x}{M},\frac{y}{M}\right) + a_{2-}\left(\frac{x}{M},\frac{y}{M}\right)\right] \qquad \textbf{(S23)}$$

Verification

Monochromatic images were acquired for a PMMA tube (diameter of 3.85 mm) with two inner tubes (diameters of 0.92 mm), made of Alumina and hydroxyapatite (HA). The corresponding imaging energies were 20 keV, 25 keV and 30 keV (Figure 1), a sample-detector of 0.6 m (z_1), an X-ray source-sample distance of 0.6, and 5 dithering steps. The objective is to retrieve the projected thickness of Alumina ($\Delta\delta(E) = \delta_{Al}(E) - \delta_{PMMA}(E)$ and $\Delta\beta(E) = \beta_{Al}(E) - \beta_{PMMA}(E)$) and HA ($\Delta\delta(E) = \delta_{HA}(E) - \delta_{PMMA}(E)$ and $\Delta\beta(E) = \beta_{HA}(E) - \beta_{PMMA}(E)$), using equations S22 and S23. The pixel size was $W = 55$ μm.

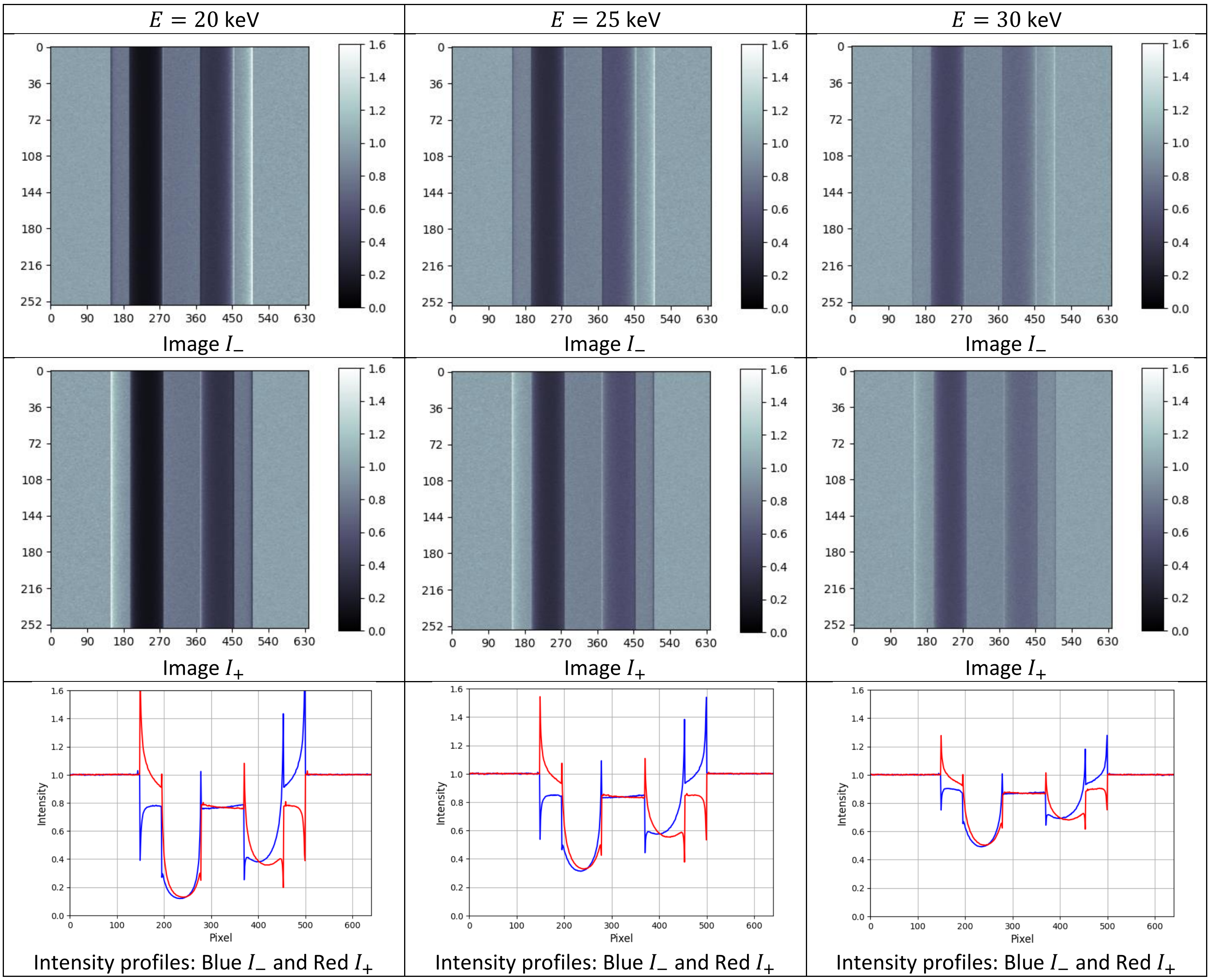

Figure 1. Images at 20, 25 and 30 keV using EISM.

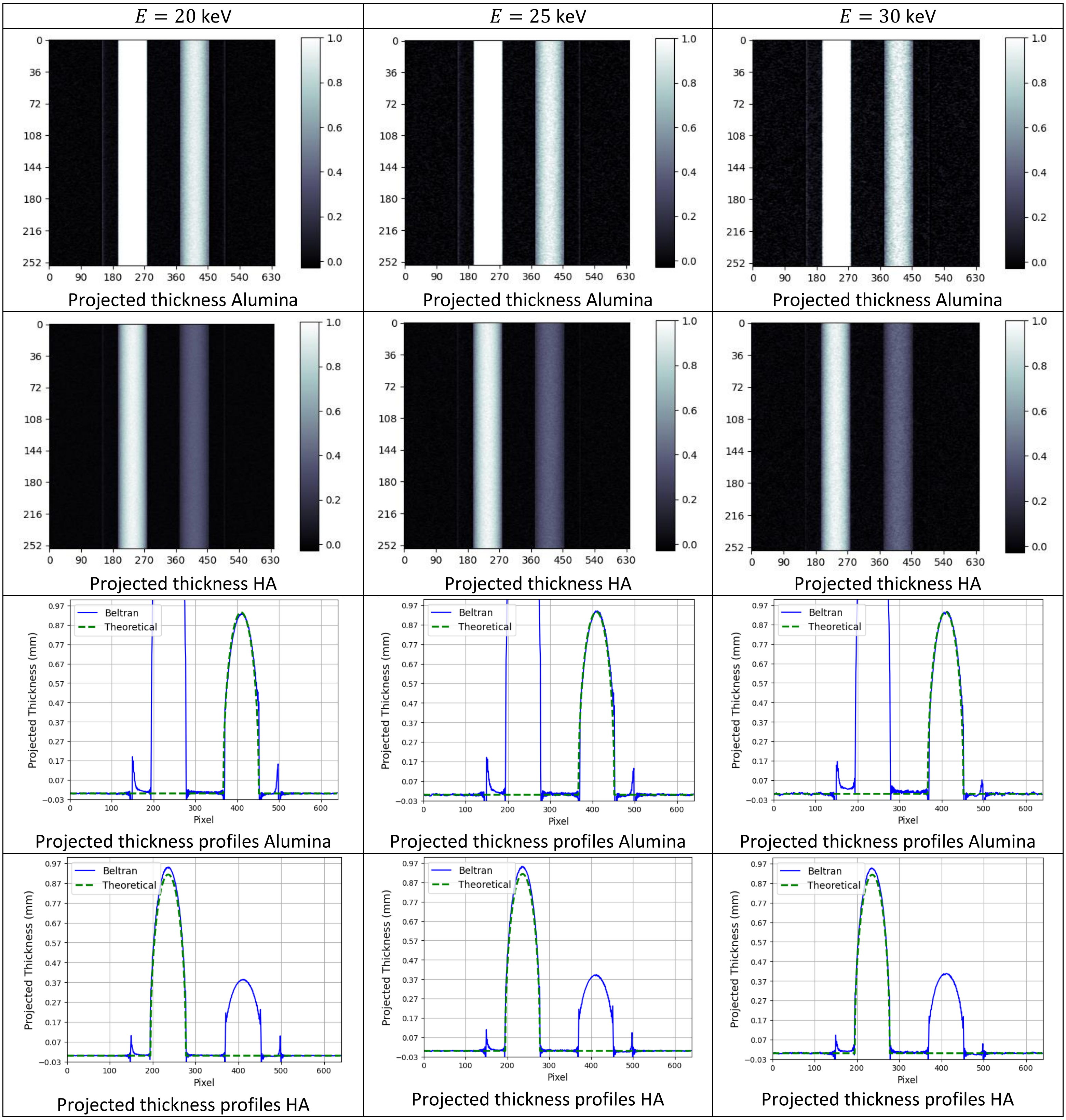

Figure 2. Projected thickness maps, with their profiles, of Alumina and HA using EISM at 20, 25 and 30 keV.

Free Propagation (Inline XPCI)

Characteristic equation: Transport-Intensity equation

$$M^2 I(x,y,z_1,E) = I\left(\frac{x}{M},\frac{y}{M},0,E\right) - \frac{z_1}{k(E)}\vec{\nabla}_T \cdot \left[I\left(\frac{x}{M},\frac{y}{M},0,E\right)\vec{\nabla}_T \phi\left(\frac{x}{M},\frac{y}{M},0,E\right)\right] \quad \textbf{(S24)}$$

$$\frac{M^2 I(x,y,z_1,E)}{I\left(\frac{x}{M},\frac{y}{M},-z_o,E\right)} = \left[e^{-2k(E)\int_{-z_o}^{0}\beta\left(\frac{x}{M},\frac{y}{M},z',E\right)dz'} + z_1\vec{\nabla}_T \cdot \left[e^{-2k(E)\int_{-z_o}^{0}\beta\left(\frac{x}{M},\frac{y}{M},z',E\right)dz'}\vec{\nabla}_T \int_{-z_o}^{0}\delta\left(\frac{x}{M},\frac{y}{M},z',E\right)dz'\right]\right] \quad \textbf{(S25)}$$

using equations S1 and S2 in equation S25.

- **Phase retrieval: Projected thickness maps**

To retrieve the projected thickness of the encapsulated material using Inline XPCI, equations S9 and S10 in equation S25 are used, again assuming $\vec{\nabla}_T a_T\left(\frac{x}{M},\frac{y}{M}\right) \approx 0$, obtaining

$$\frac{M^2 I(x,y,z_1,E)}{I\left(\frac{x}{M},\frac{y}{M},-z_o,E\right)e^{-2k(E)\beta_1(E)a_T\left(\frac{x}{M},\frac{y}{M}\right)}} = e^{-2k(E)\Delta\beta(E)a_2\left(\frac{x}{M},\frac{y}{M}\right)} + z_1\Delta\delta(E)\vec{\nabla}_T \cdot \left[e^{-2k(E)\Delta\beta(E)a_2\left(\frac{x}{M},\frac{y}{M}\right)}\vec{\nabla}_T a_2\left(\frac{x}{M},\frac{y}{M}\right)\right]$$

$$\frac{M^2 I(x,y,z_1,E)}{I\left(\frac{x}{M},\frac{y}{M},-z_o,E\right)e^{-2k(E)\beta_1(E)a_T\left(\frac{x}{M},\frac{y}{M}\right)}} = \left[1 - \frac{z_1\Delta\delta(E)}{2k(E)\Delta\beta(E)}\nabla_T^2\right]e^{-2k(E)\Delta\beta(E)a_2\left(\frac{x}{M},\frac{y}{M}\right)} \quad \textbf{(S26)}$$

where $\vec{\nabla}_T e^{-2k(E)\Delta\beta(E)a_2\left(\frac{x}{M},\frac{y}{M}\right)} = -2k(E)\Delta\beta(E)e^{-2k(E)\Delta\beta(E)a_2\left(\frac{x}{M},\frac{y}{M}\right)}\vec{\nabla}_T a_2\left(\frac{x}{M},\frac{y}{M}\right)$. Using discrete Fourier space enables to convert the differential equation S26 into an algebraic equation. The discrete Fourier transforms of each function from equation S26 are

$$F(x,y,E) = \frac{M^2 I(x,y,z_1,E)}{I\left(\frac{x}{M},\frac{y}{M},-z_o,E\right)e^{-2k(E)\beta_1(E)a_T\left(\frac{x}{M},\frac{y}{M}\right)}} = \frac{1}{N^2}\sum_{u,v=-\frac{N}{2}}^{\frac{N}{2}} f(u,v,E)e^{\frac{2\pi i}{N}(xu+yv)} \quad \textbf{(S27)}$$

$$G(x,y,E) = e^{-2k(E)\Delta\beta(E)a_2\left(\frac{x}{M},\frac{y}{M}\right)} = \frac{1}{N^2}\sum_{u,v=-\frac{N}{2}}^{\frac{N}{2}} g(u,v,E)e^{\frac{2\pi i}{N}(xu+yv)} \quad \textbf{(S28)}$$

For the Laplacian of the function G, it is considered

$$\nabla_T^2 G(x,y,E) = \frac{\partial^2 G(x,y,E)}{\partial x'^2} + \frac{\partial^2 G(x,y,E)}{\partial y'^2} \quad \textbf{(S29)}$$

A second-order Taylor expansion around the center of mass of an arbitrary pixel (x,y) is used to calculate the function G at the center of mass of its nearest neighboring pixels, at $(x \pm W, y)$ and $(x, y \pm W)$, and to calculate the discrete second derivatives of G as

$$G(x \pm W, y, E) = G(x,y,E) \pm W \frac{\partial G(x,y,E)}{\partial x'} + \frac{W^2}{2}\frac{\partial^2 G(x,y,E)}{\partial x'^2} \tag{S30}$$

$$\frac{\partial^2 G(x,y,E)}{\partial x'^2} = \frac{1}{W^2}[G(x+W,y,E) + G(x-W,y,E) - 2G(x,y,E)] \tag{S31}$$

$$G(x, y \pm W, E) = G(x,y,E) \pm W \frac{\partial G(x,y,E)}{\partial y'} + \frac{W^2}{2}\frac{\partial^2 G(x,y,E)}{\partial y'^2} \tag{S32}$$

$$\frac{\partial^2 G(x,y,E)}{\partial y'^2} = \frac{1}{W^2}[G(x,y+W,E) + G(x,y-W,E) - 2G(x,y,E)] \tag{S33}$$

$$\nabla_T^2 G(x,y,E) = \frac{1}{W^2}[G(x+W,y,E) + G(x-W,y,E) + G(x,y+W,E) + G(x,y-W,E) - 4G(x,y,E)] \tag{S34}$$

$$\begin{aligned}\nabla_T^2 G(x,y,E) = \frac{1}{W^2N^2}\Bigg[&\sum_{u,v=-\frac{N}{2}}^{\frac{N}{2}}\left[e^{\frac{2\pi i}{N}Wu} + e^{-\frac{2\pi i}{N}Wu}\right] g(u,v,E) e^{\frac{2\pi i}{N}(xu+yv)} \sum_{u,v=-\frac{N}{2}}^{\frac{N}{2}}\Big[e^{\frac{2\pi i}{N}Wv} \\ &+ e^{-\frac{2\pi i}{N}Wv}\Big] g(u,v,E) e^{\frac{2\pi i}{N}(xu+yv)} - \sum_{u,v=-\frac{N}{2}}^{\frac{N}{2}} 4g(u,v,E) e^{\frac{2\pi i}{N}(xu+yv)}\Bigg]\end{aligned} \tag{S36}$$

$$\nabla_T^2 G(x,y,E) = \frac{1}{N^2}\sum_{u,v=-\frac{N}{2}}^{\frac{N}{2}} \frac{2}{W^2}\left[\cos\left(\frac{2\pi Wu}{N}\right) + \cos\left(\frac{2\pi Wv}{N}\right) - 2\right] g(u,v,E) e^{\frac{2\pi i}{N}(xu+yv)} \tag{S37}$$

With equations S27, S28 and S37, equation S26 is expressed as

$$\begin{aligned}&\frac{1}{N^2}\sum_{u,v=-\frac{N}{2}}^{\frac{N}{2}} f(u,v,E) e^{\frac{2\pi i}{N}(xu+yv)} \\ &= \frac{1}{N^2}\sum_{u,v=-\frac{N}{2}}^{\frac{N}{2}}\left[1 - \frac{z_1 \Delta\delta(E)}{W^2 k(E)\Delta\beta(E)}\left[\cos\left(\frac{2\pi Wu}{N}\right) + \cos\left(\frac{2\pi Wv}{N}\right) - 2\right]\right] g(u,v,E) e^{\frac{2\pi i}{N}(xu+yv)}\end{aligned}$$

$$f(u,v,E) = \left[1 - \frac{z_1 \Delta\delta(E)}{W^2 k(E)\Delta\beta(E)}\left[\cos\left(\frac{2\pi Wu}{N}\right) + \cos\left(\frac{2\pi Wv}{N}\right) - 2\right]\right] g(u,v,E) \tag{S38}$$

$$g(u,v,E) = \frac{f(u,v,E)}{1 - \frac{z_1 \Delta\delta(E)}{W^2 k(E)\Delta\beta(E)}\left[\cos\left(\frac{2\pi Wu}{N}\right) + \cos\left(\frac{2\pi Wv}{N}\right) - 2\right]} \tag{S39}$$

allowing to estimate $a_2\left(\frac{x}{M},\frac{y}{M}\right)$ from $g(u,v,E)$ in equation S28 as

$$e^{-2k(E)\Delta\beta(E)a_2\left(\frac{x}{M},\frac{y}{M}\right)} = \frac{1}{N^2}\sum_{u,v=-\frac{N}{2}}^{\frac{N}{2}}\left[\frac{f(u,v,E)}{1 - \frac{z_1 \Delta\delta(E)}{W^2 k(E)\Delta\beta(E)}\left[\cos\left(\frac{2\pi Wu}{N}\right) + \cos\left(\frac{2\pi Wv}{N}\right) - 2\right]}\right] e^{\frac{2\pi i}{N}(xu+yv)}$$

$$a_2\left(\frac{x}{M},\frac{y}{M}\right) = -\frac{1}{2k(E)\Delta\beta(E)}\ln\left[\frac{1}{N^2}\sum_{u,v=-\frac{N}{2}}^{\frac{N}{2}}\left[\frac{f(u,v,E)}{1-\frac{z_1\Delta\delta(E)}{W^2k(E)\Delta\beta(E)}\left[\cos\left(\frac{2\pi Wu}{N}\right)+\cos\left(\frac{2\pi Wv}{N}\right)-2\right]}\right]e^{\frac{2\pi i}{N}(xu+yv)}\right] \quad \textbf{(S40)}$$

Verification

Monochromatic images were acquired for a PMMA tube (diameter of 3.85 mm) with two inner tubes (diameters of 0.92 mm), made of Alumina and hydroxyapatite (HA). The corresponding imaging energies were 20 keV, 25 keV and 30 keV (Figure 3), a sample-detector of 0.6 m (z_1), and an X-ray source-sample distance of 0.6. The objective is to retrieve the projected thickness of Alumina ($\Delta\delta(E) = \delta_{Al}(E) - \delta_{PMMA}(E)$ and $\Delta\beta(E) = \beta_{Al}(E) - \beta_{PMMA}(E)$) and HA ($\Delta\delta(E) = \delta_{HA}(E) - \delta_{PMMA}(E)$ and $\Delta\beta(E) = \beta_{HA}(E) - \beta_{PMMA}(E)$), using equation S40. The pixel size was $W = 55\ \mu$m.

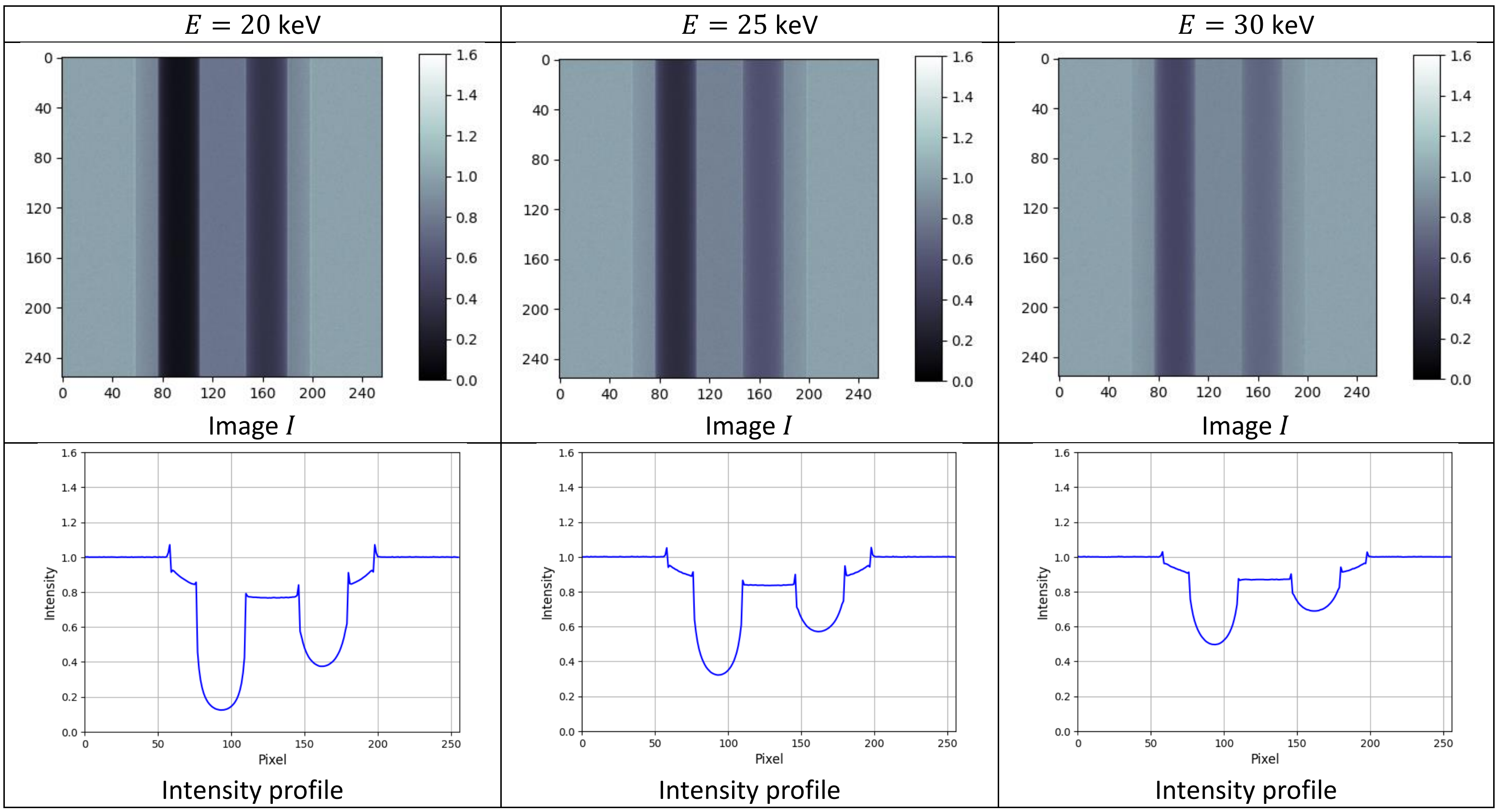

Figure 3. Images at 20, 25 and 30 keV using Inline XPCI.

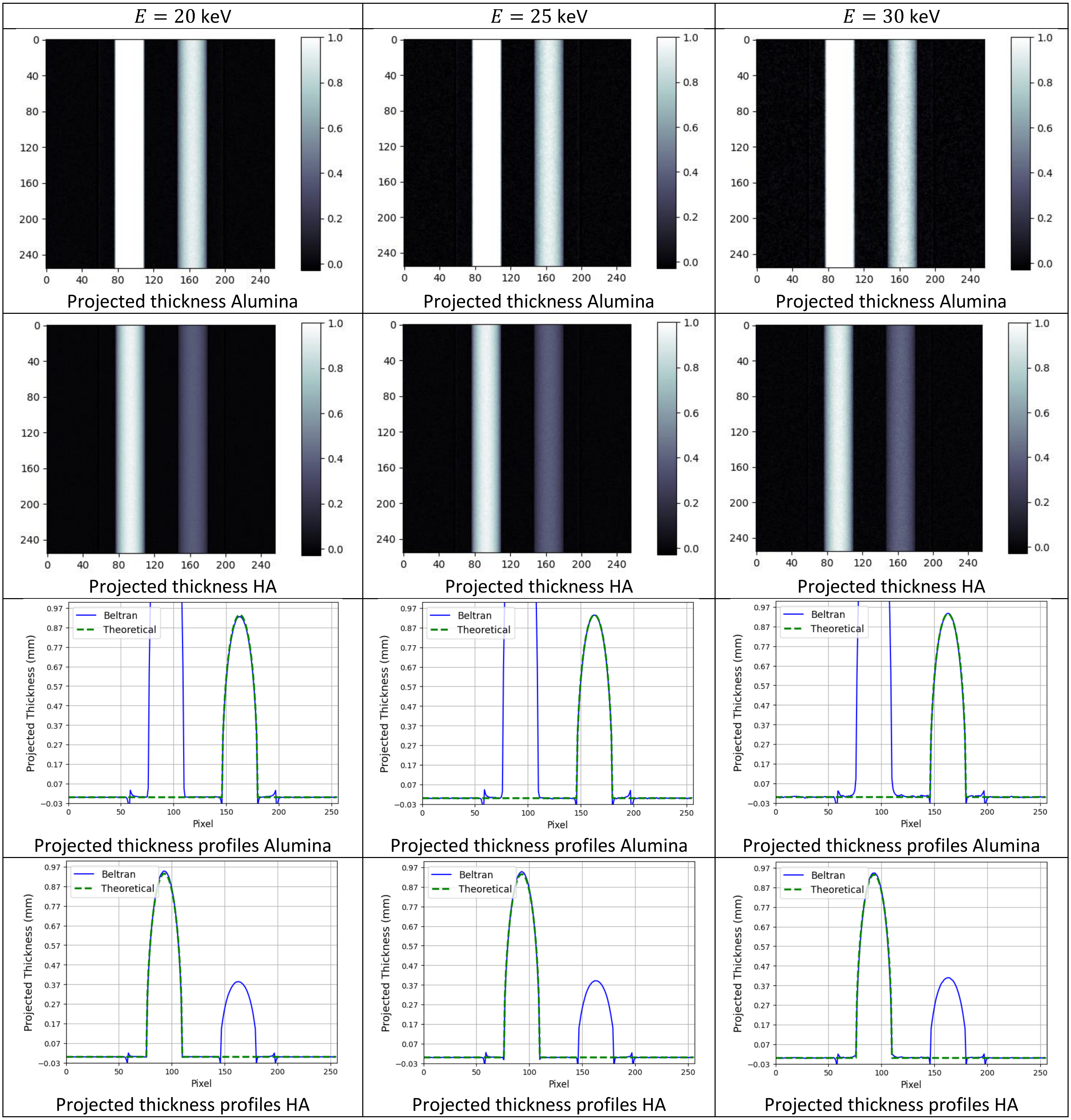

Figure 4. Projected thickness maps, with their profiles, of Alumina and HA using Inline XPCI at 20, 25 and 30 keV.